



Recent Progress on Structural Health Monitoring by Fibre Optic Sensor In Civil Engineering

Hong-Nan LI, Liang Ren

*State Key Laboratory of Coastal and Offshore Engineering, School of
Civil and Hydraulic Engineering*

Dalian University of Technology, Dalian 116023, China



Outline

- Disasters
- Structural Health Monitoring System
- Background of Structural Health Monitoring
- Development of fibre optic sensors
- Fibre optic sensor applications in related fields
- Current status of fibre optic sensors
- Recent applications in civil engineering
- Summary



Disasters



World trade center



Kobe earthquake

Northridge earthquake



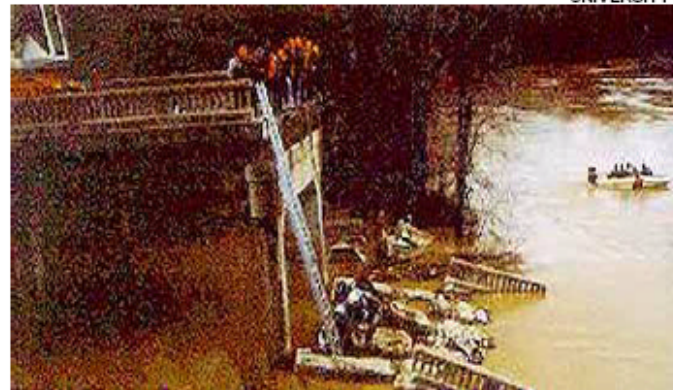


Structural Health Monitoring

CASE STUDY



Collapse of NY Thruway (I-90) Bridge (1987)
Schoharie Creek



The Hatchie River Bridge failure Covington, TENN, 1989

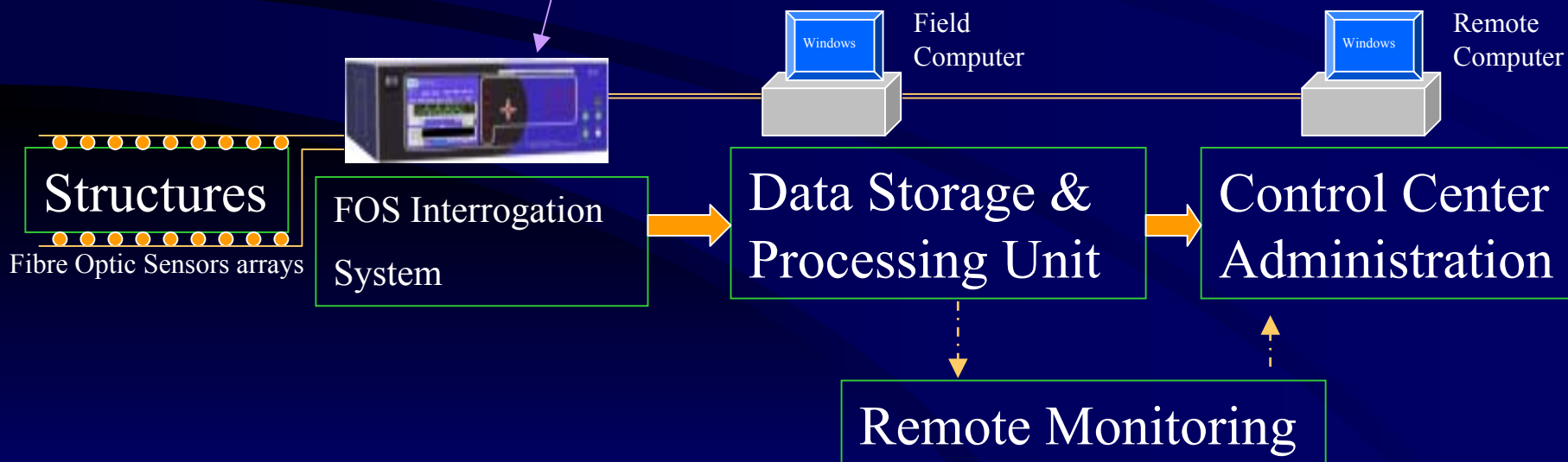
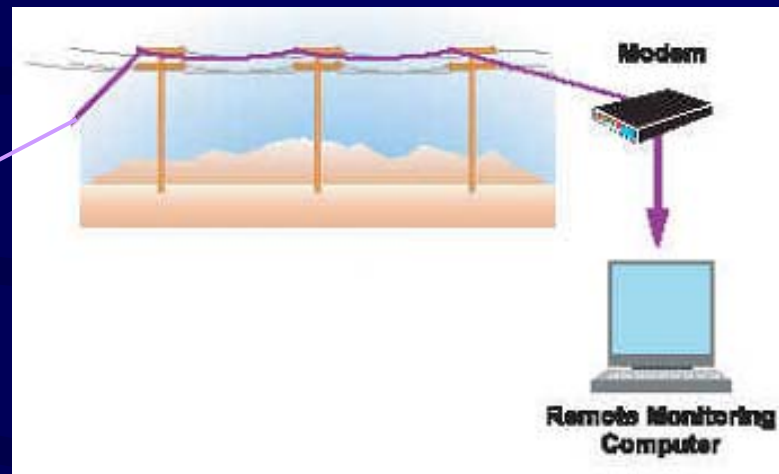


During 1987-2000, there have been 31 collapses of such bridges in NY state. Most of them had been caused by "external factors" like trucks exceeding the posted weight limits or crashing into bridges.

◀ The Mianus River Bridge collapse
Greenwich, CONN, 1983



Structural Health Monitoring System





Health Monitoring Contents

Structures

1. Existence of Damage
2. Location of Damage
3. Severity of Damage
4. Life of the structures

Monitoring

- Acceleration
- Displacement
- Pressure
- Temperature

Health: or Not



Interior/Body
Cracks

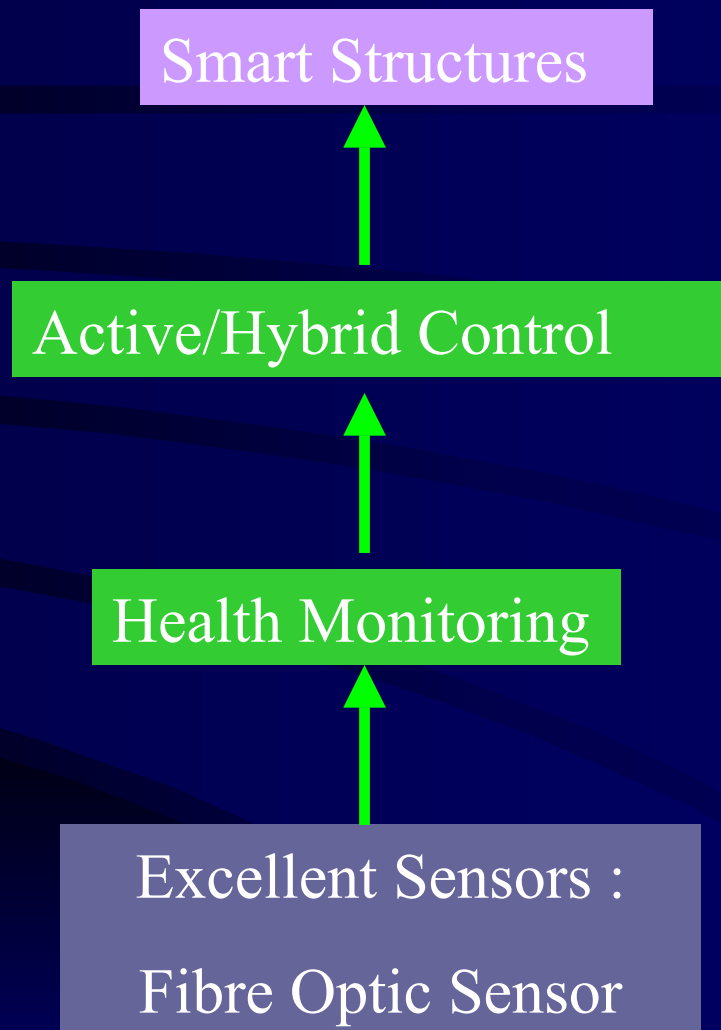
\neq

Exterior/Surface
Parameters

Fibre Optic Sensors: Embeddible and Attachable




Health Monitoring → Smart Structures





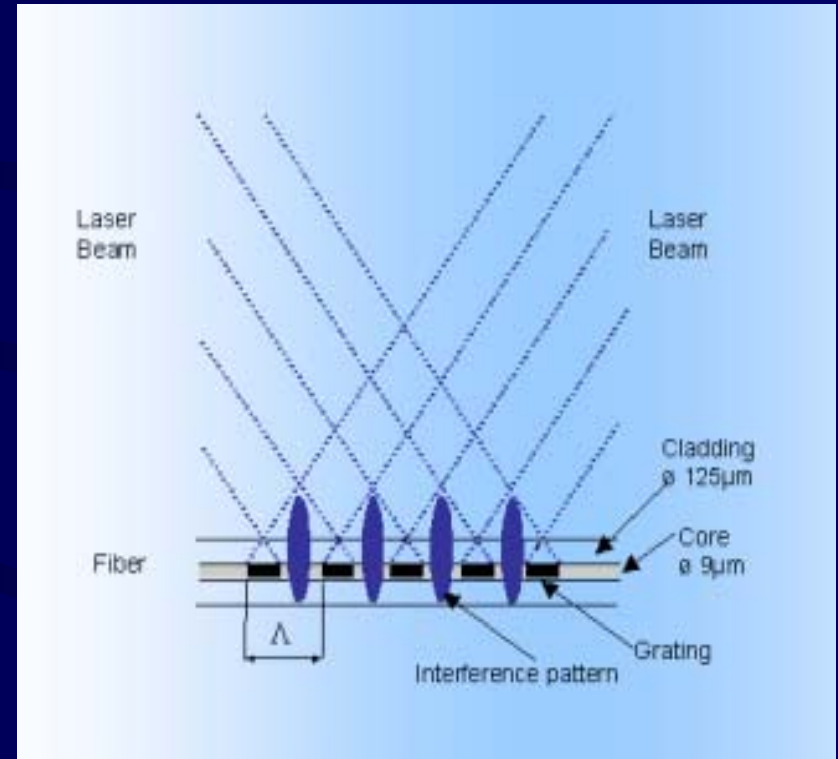
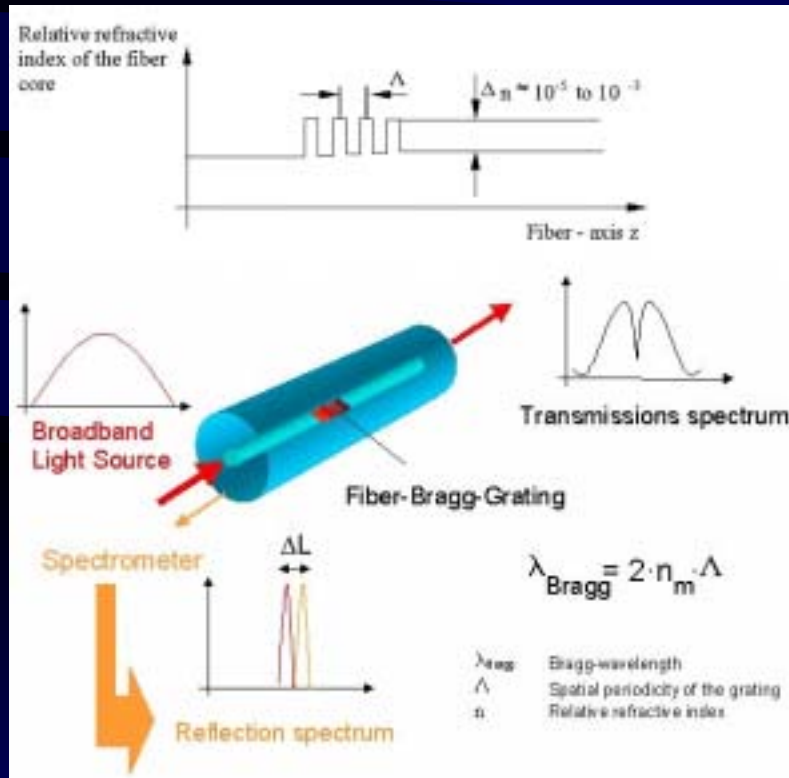
History of FBG

- Hill *et al.* in 1978 at Canadian Communications Research Centre(CRC)  by Standing Wave Pattern. *Gratings:* Reflection filter
- Meltz *et al.* in 1989, USA. By transverse holographic method.
- Hill *et al.* in 1993 at (CRC) by Phase Mask.



Quasi Distributed FBG Sensors

Principle

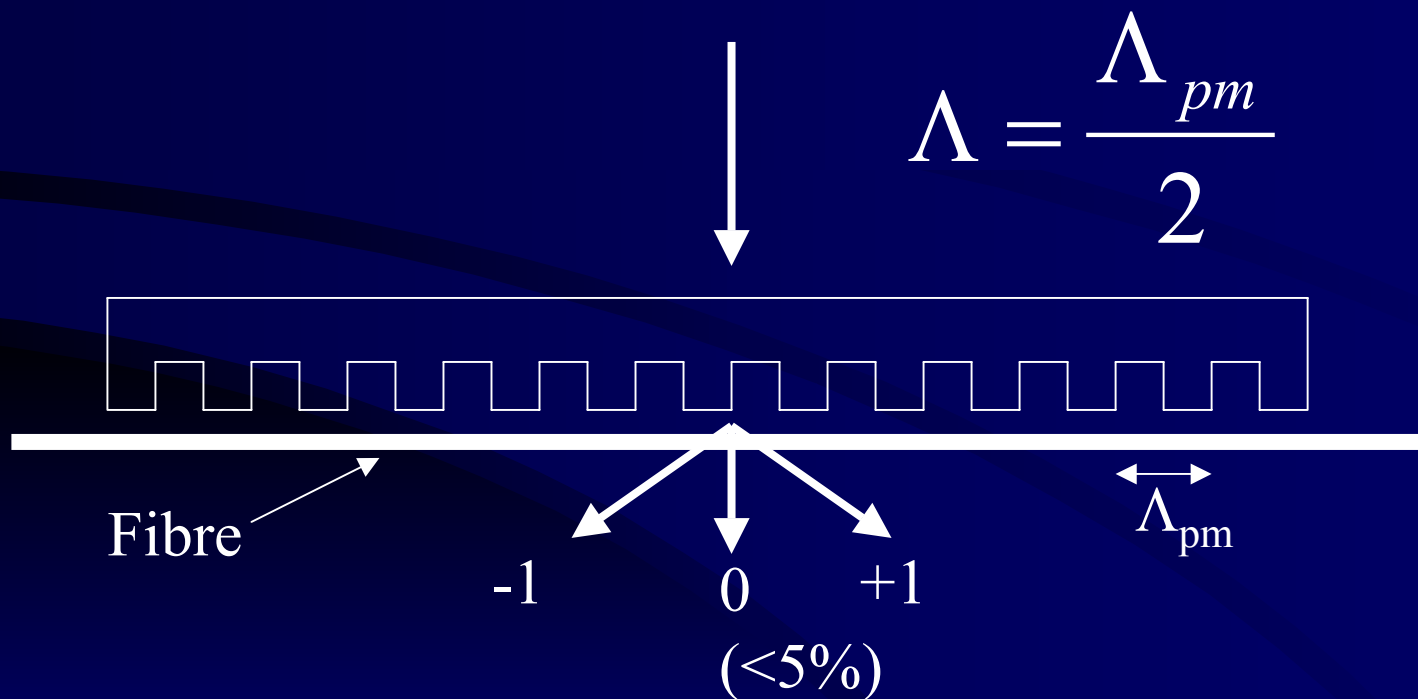


Phase Mask
Forming



Phase Mask

- Most of the diffraction contained in the 0th, 1st.
 - Need to block 0th order by controlling the depth of the corrugations in the phase mask.



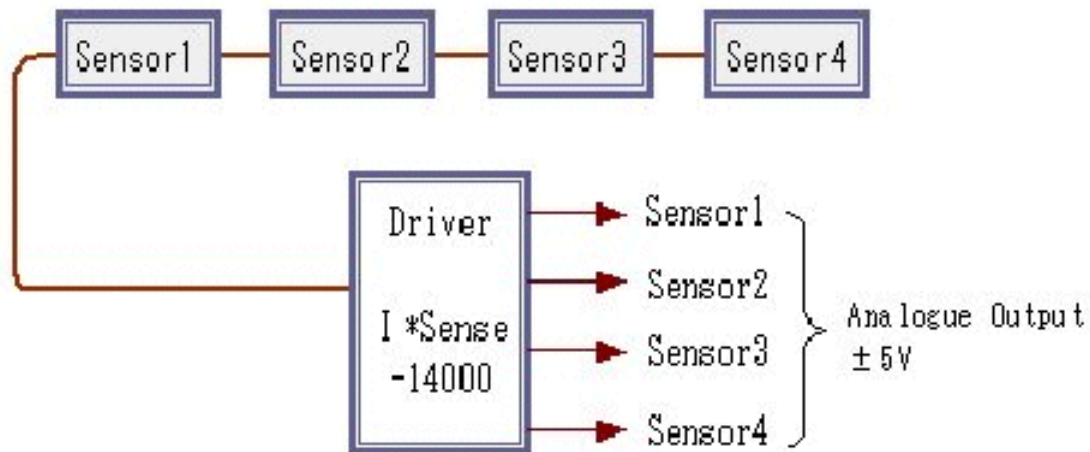


FBG Sensors Interrogation Systems



Figure 4. Micron Optics, Inc. FBG-IS Demodulation Unit with Laptop PC Interface

DRIVER for FBG Sensor





FBG temperature sensor

To a bare FBG, at $\lambda_B = 1520-1570\text{nm}$

$$\partial\lambda_B/\partial T = 10.8\text{pm}/^\circ\text{C}$$

But

$$\partial\lambda_B/\partial\varepsilon = 1.2\text{pm}/\mu\varepsilon$$

It is **important** to reduce the adverse effect of strain availably and improve the thermal sensitivity remarkably.



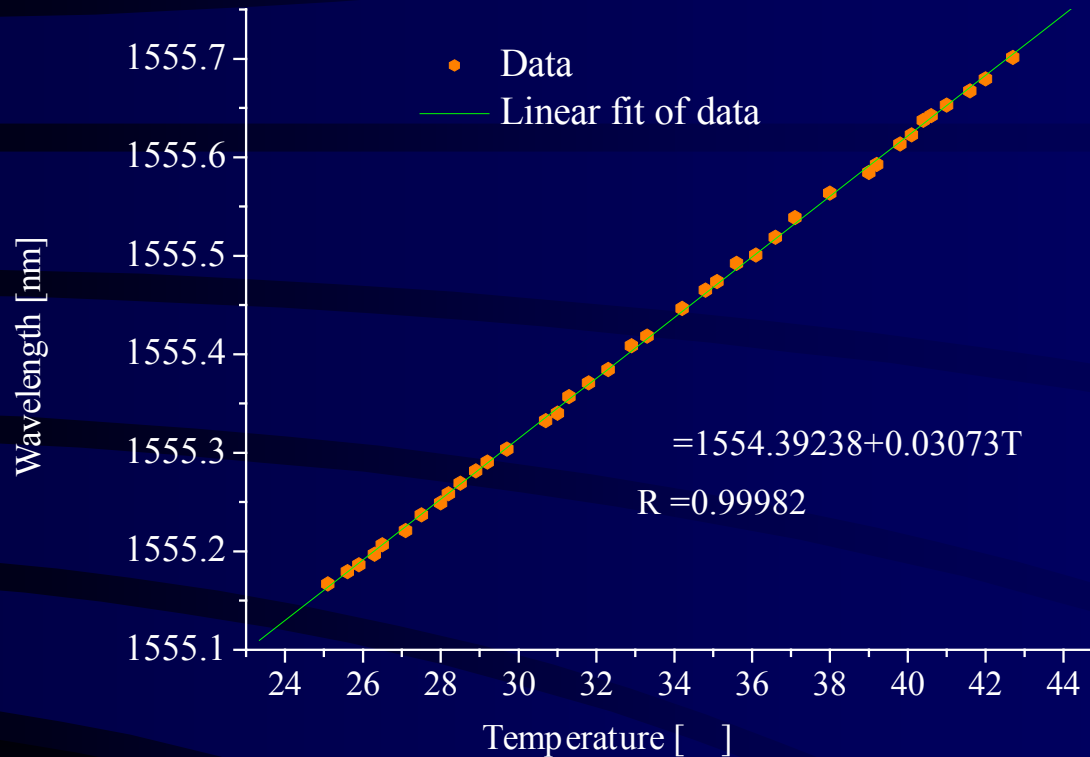
Sensor design



Picture of stainless steel tube-packaged FBG sensor.



Sensitivity of sensor



- The sensitivity can reach **30.73 pm/°C**
- The measurement precision exceeds **±0.1**



FBG strain sensor



Picture of stainless steel tube-packaged FBG strain sensor.



Sensitivity of sensor

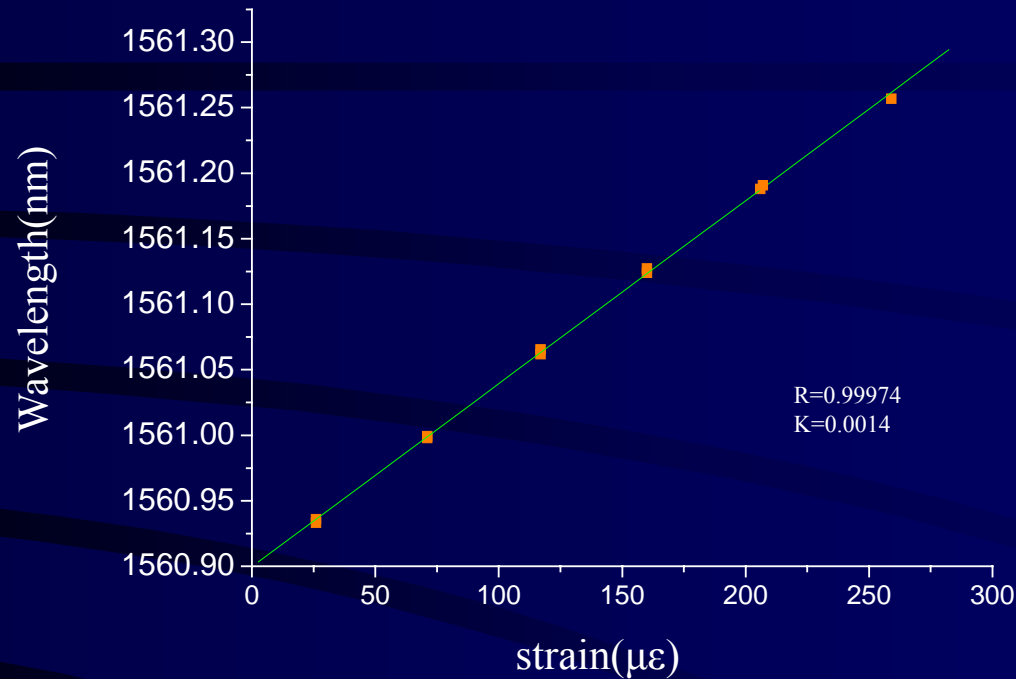


Fig. 6. Relationship between wavelength variation of FBG strain sensor and strain



Advances of structural health monitoring using fiber Bragg grating in our group

- Application of FBG temperature sensors to ground heat pump system
- Experiment study on strain monitoring of concrete during cure period with FBG sensors
- Application of FBG sensors in the vibration experiment of submarine pipeline model
- Experiments on an offshore platform by FBG sensors



Application of FBG temperature sensors to ground heat pump system

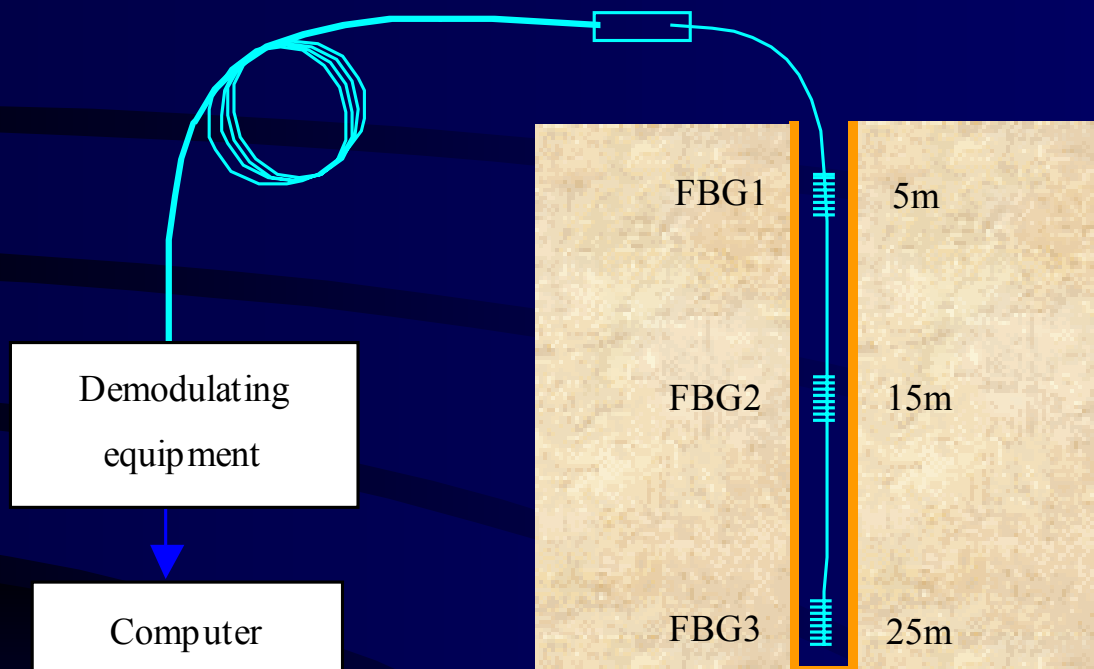


Fig. 3. Schematic diagram of 3 channels FBG sensor system.



Pipe line

Well

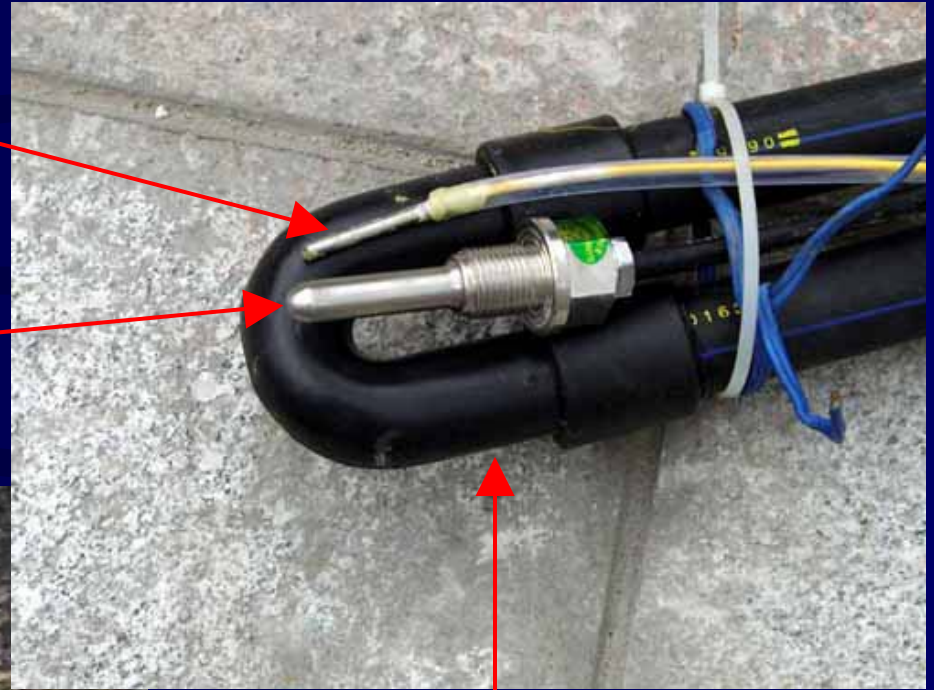


Fiber cable



FBG sensor

Thermal resistance



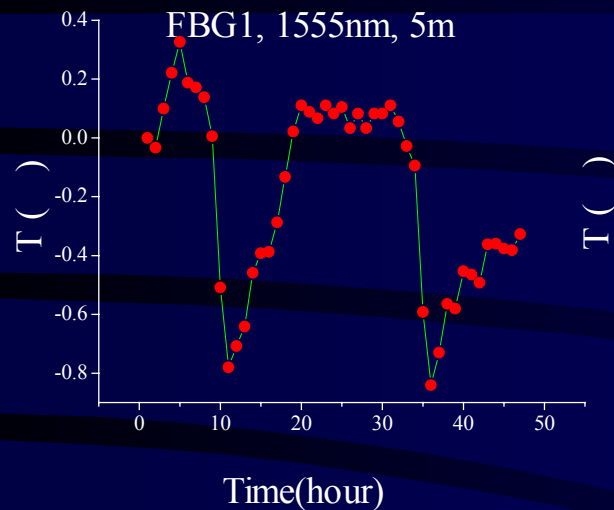
Pipe line



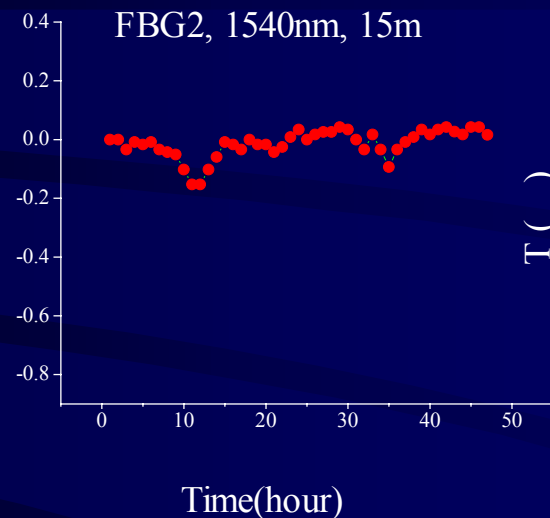
Installation



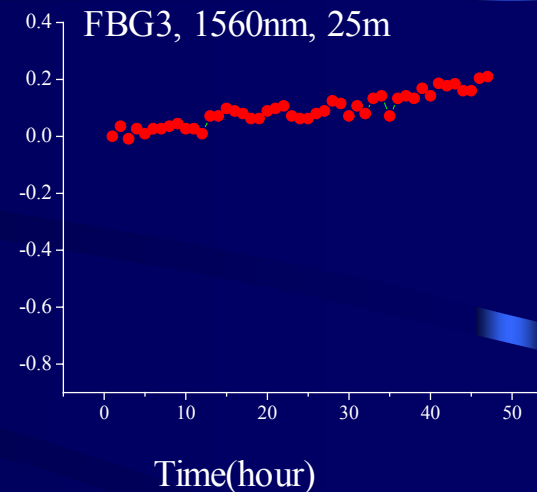
Experimental result (1)



(A)



(B)



(C)

Fig. 4. Temperature variation of FBG sensors in 48 hours.



Experimental result (1)

- The fluctuation of temperature decreases with the increasing depth of sensor's location.
- Though it was autumn, the temperature underground was still increasing slowly.



Experimental result (2)

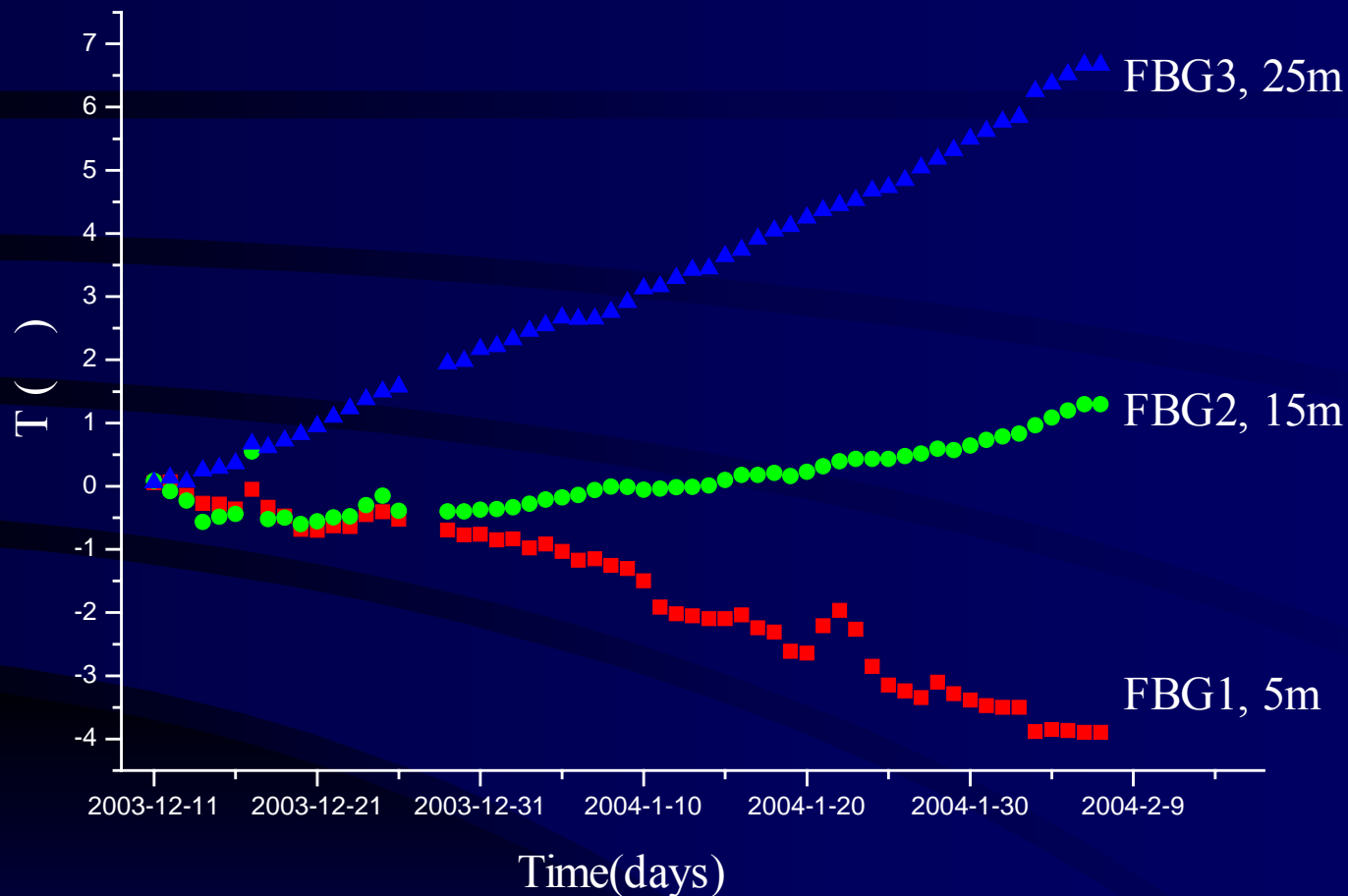


Fig. 5. Temperature shift of FBG sensors in two months.



Experiment study on strain monitoring of concrete during cure period with FBG sensors

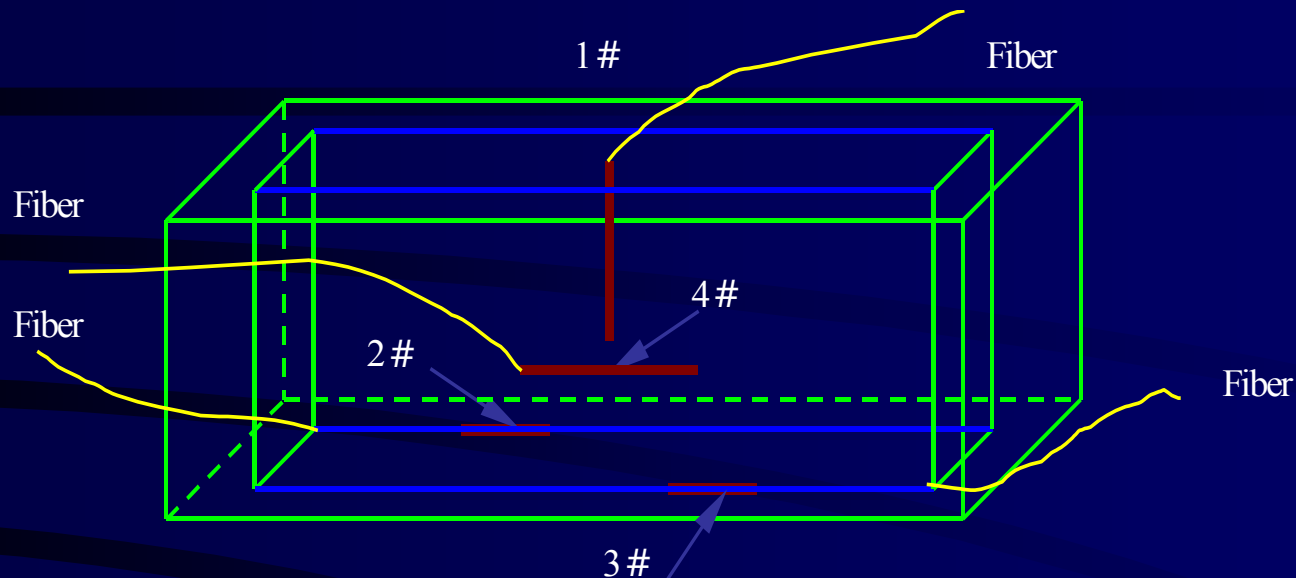
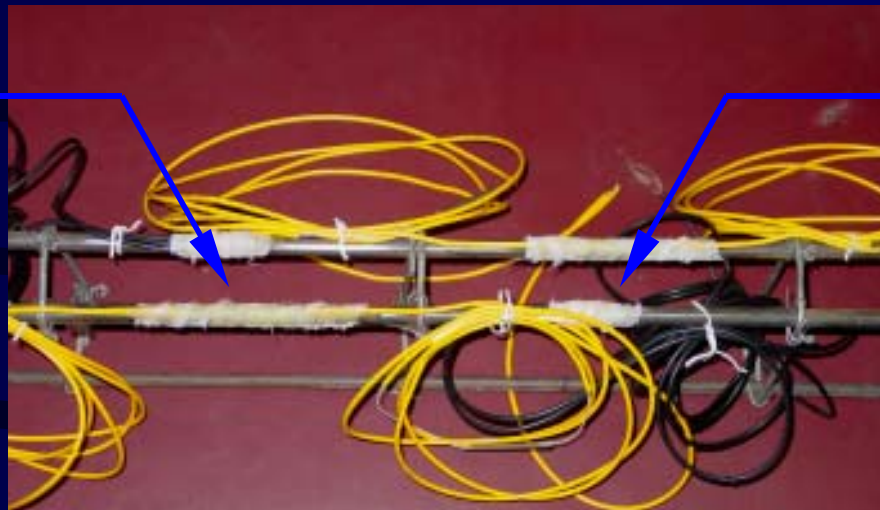


Fig. 10. Figure of sensors embedded in concrete

Number	Types of sensor	Wavelength (nm)	Position of sensor
1 #	FBG temperature sensor	1525	In concrete
2 #	FBG strain sensor	1540	On longitudinal bar
3 #	Bare FBG sensor	1540	On longitudinal bar
4 #	FBG strain sensor	1531	In concrete



2 # FBG strain
sensor



3 # bare FBG
sensor

Fig. 11 The picture of sensors installed on bar

The monitoring time of this experiment is from **3rd** hour to **16th** hour after pouring.



At **9th hour** after pouring, the temperature of concrete reach the highest value, and then it decreases slowly. The **total temperature shift** is about **2** .

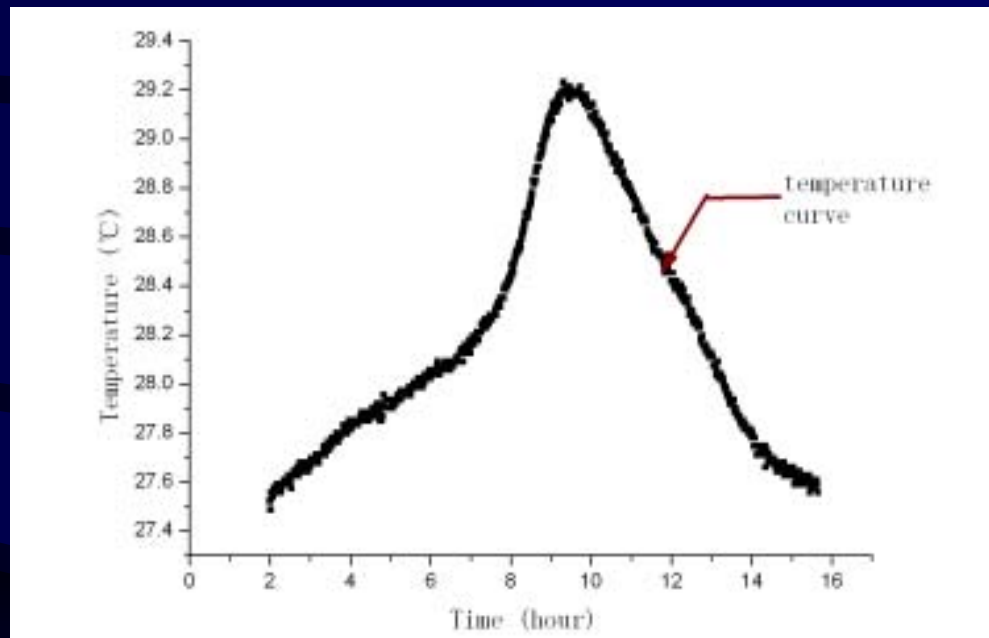
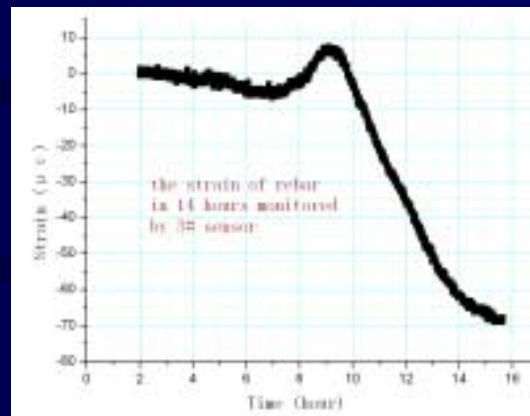
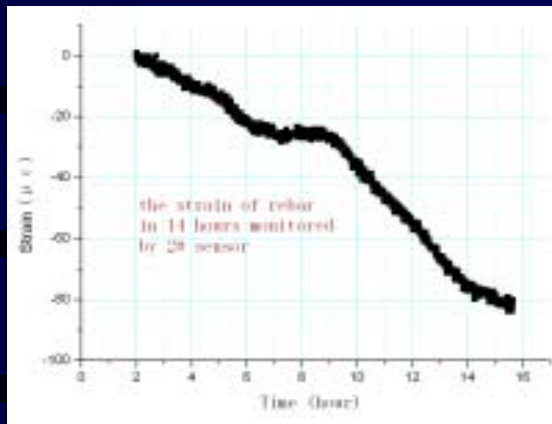


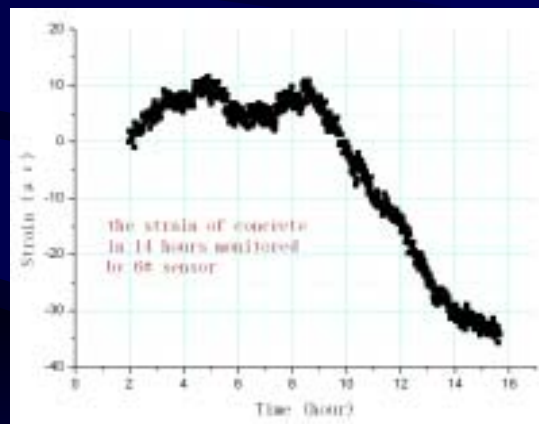
Fig.12. Temperature curve of concrete in the cure period



Strain shift



Sensors on the **bar**

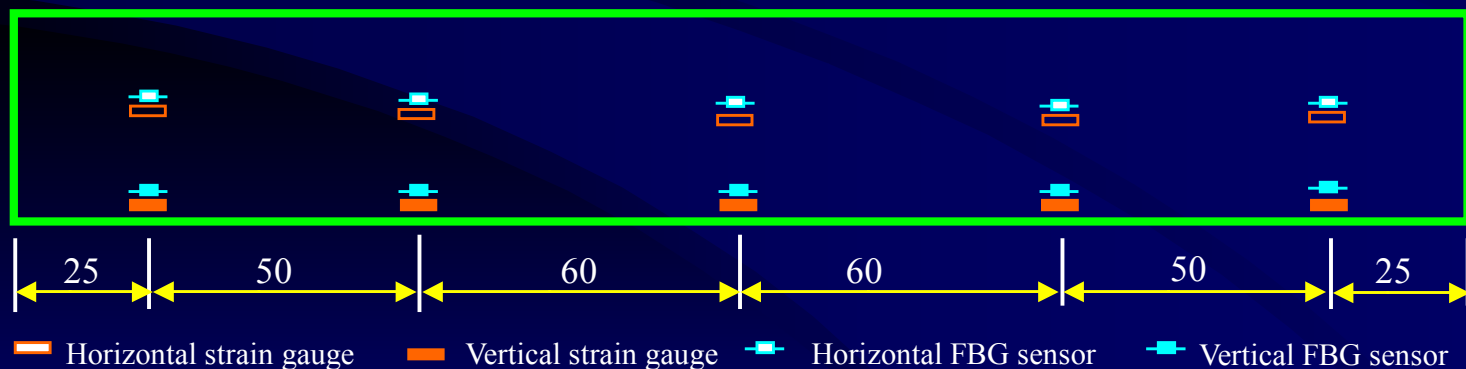


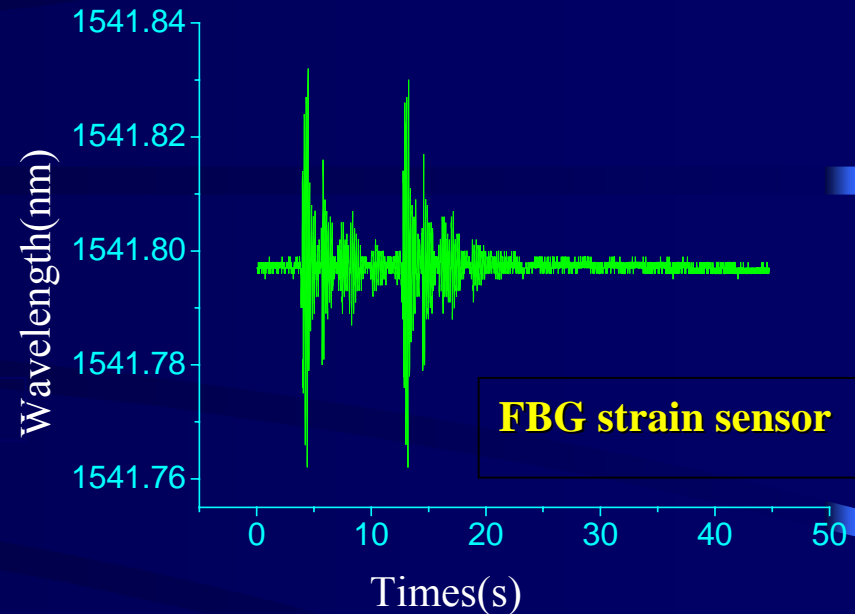
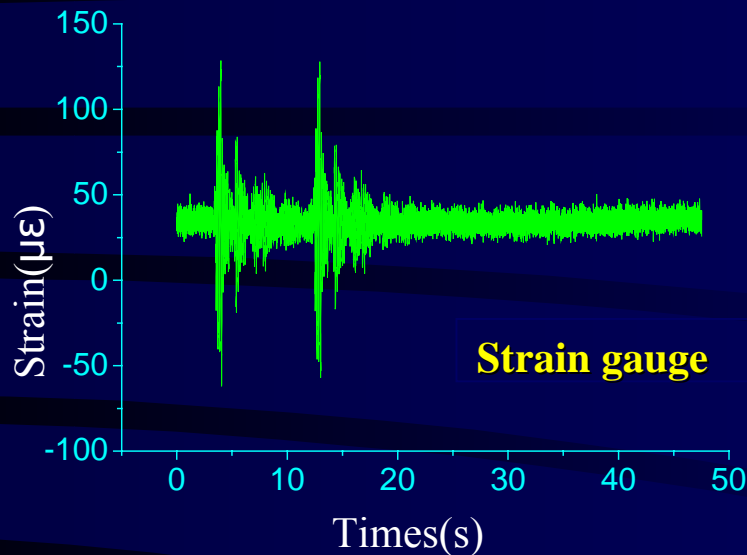
Sensors in the **concrete**

Fig. 13 Strain of rebar monitored by 2#, 3# and 4# sensor



Application of FBG sensors in the vibration experiment of submarine pipeline model





For the electromagnetic interference of environment, the noise of electric strain gauge is about **$25\mu\epsilon$** . It is much greater than the noise of FBG sensor that is only **$4\mu\epsilon$** .



Experiments on an offshore platform model by FBG sensors

Fig. 16. Model of the single post offshore platform in the direction of east to west



Table 2. Sensor specifications

Demodulation unit channel No.	1	1	1	1	2
Sensor No.	Sensor 1	Sensor 2	Sensor 3	Sensor 4	Sensor 5(BPS-701)
FBG Serial No.	519004	519016	Z6166	520012	30043
Central wavelength (nm)	1530	1556	1560	1535	1542
Type of sensor	Temperature	Strain	Strain	Strain	Accelerator

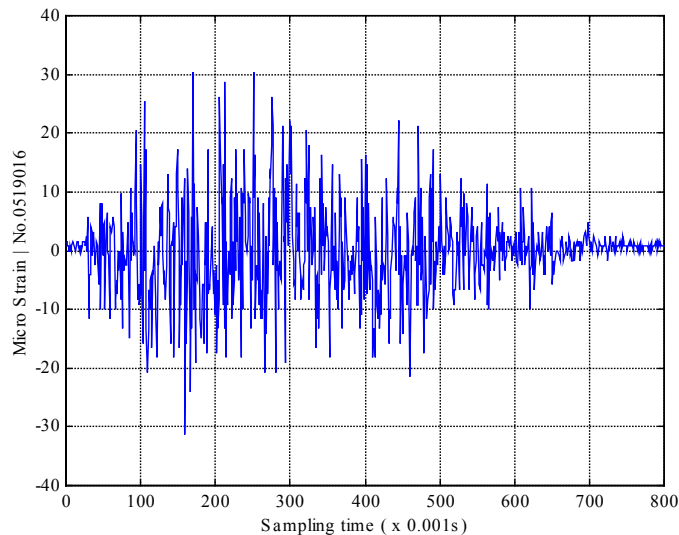


Fig.18. Dynamic acceleration response for design input spectrum.

Fig.19. Power density spectrum of the acceleration responses of the platform for sine excitations

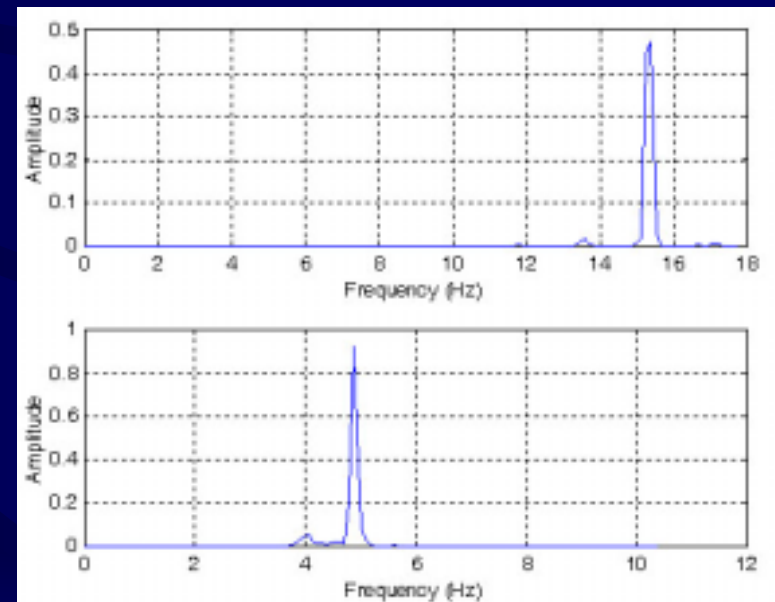




Fig.20. Model of the single post offshore platform immersed in water in the direction of east to west

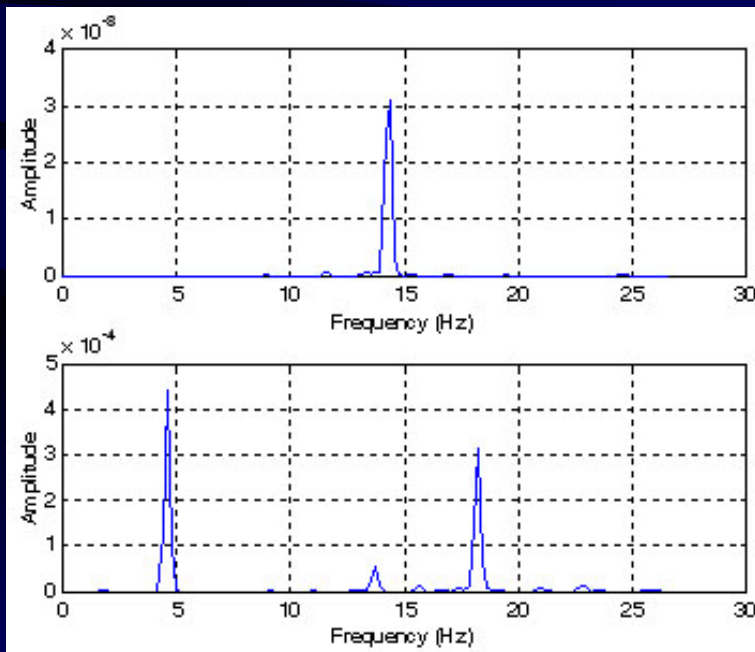


Fig.21. Power density spectrum of the acceleration responses of the platform for sine excitations when immersed in water



Strain monitoring in the oil production offshore platform

FBG strain sensors were applied in strain monitoring of oil production offshore platform No.CB271, located in Yellow Sea, whose model is presented before.



Fig. 22. Sensors installation in oil production platform



Fig.23. The platform picture and sensors position



Ship impact position

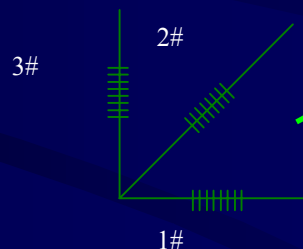
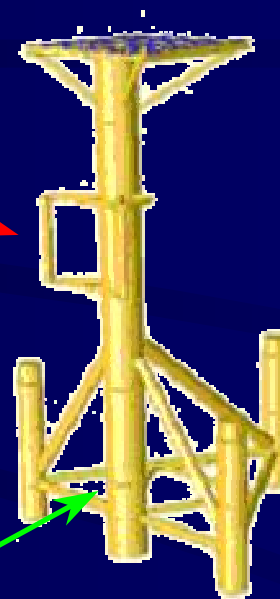


Fig. 23 shows a strain course induced by an impaction of ship with hundreds tons weight

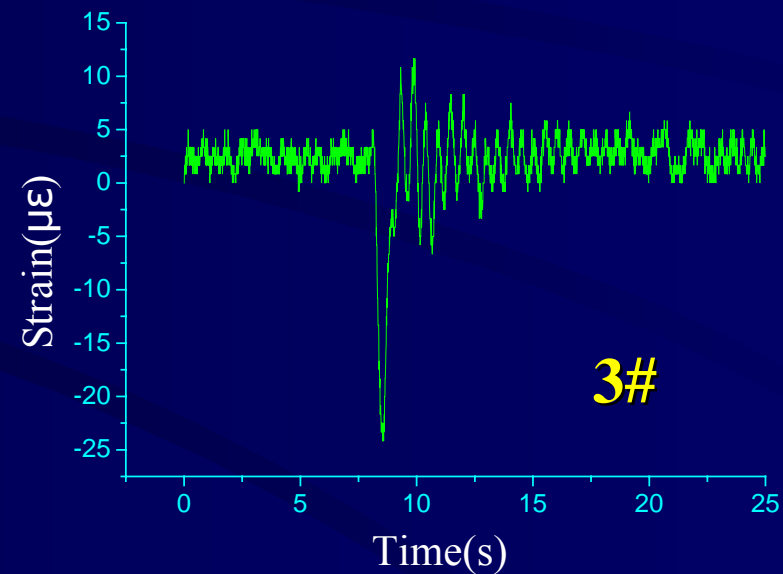
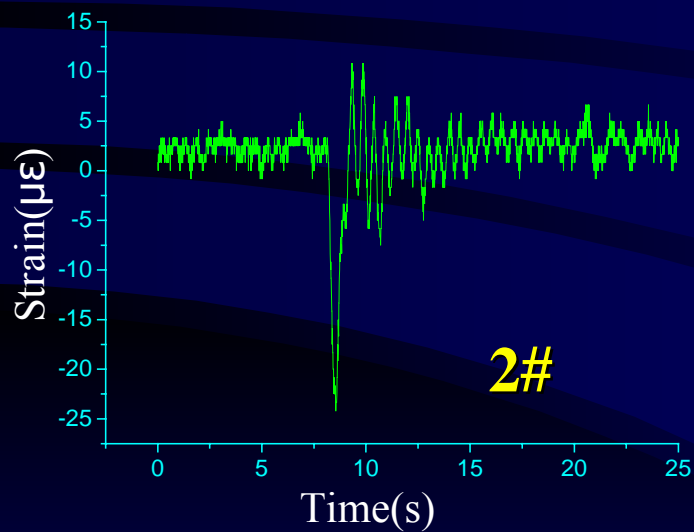
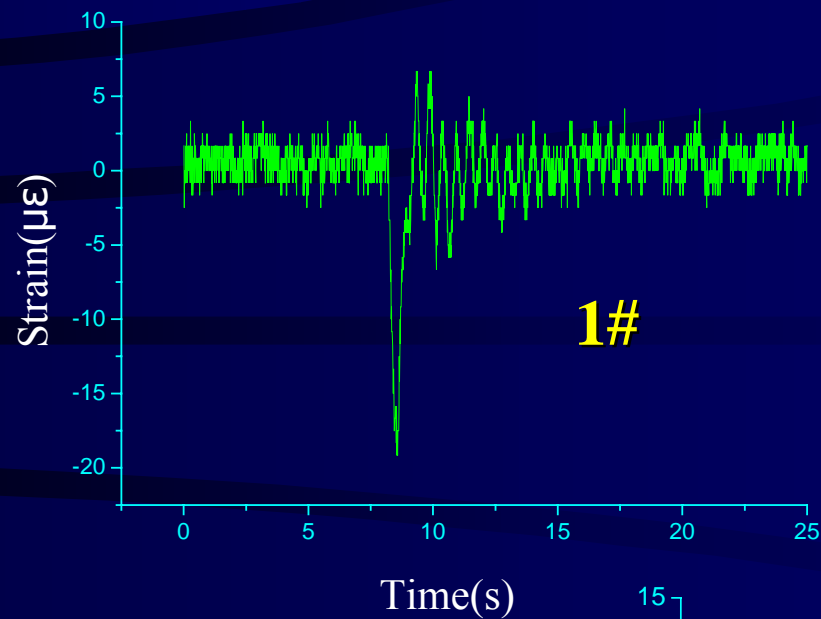


Fig.24. Strain course induced by ship impactation by embedded FBG stain sensor



Strain monitoring in architecture engineering



12 FBG sensors were installed in monitoring the strain and temperature variation of reservoir architecture underground.



Fiber cable pipeline



Temperature sensor

Strain sensor



FBG sensors in the pillar

FBG sensors in the girder

8 FBG sensors were installed in the girder and pillar



Bar dressing

Temperature sensor

FBG sensors installation

Strain sensor





Summary

Fiber optic sensors for health monitoring in Civil Engineering
fully potential

- Advantages:

- Long life durability
- High temperature endurance
- EMI immunity and noise free
- Flexibility and embeddability due to small size
- Their multiplexity

Smart structures and intelligent systems



Summary

Challenges and Problems:

- Packing
- Temperature and strain discrimination
- Ingress/Egress
- Integration of FOS and structural system
- Prices



THANK YOU FOR ATTENTION



2002年12月

Hong-Nan Li, *SHM by FOS in Civil Engineering*

